Arabian Journal of Chemistry (2022) **15**, 103942

King Saud University

Arabian Journal of Chemistry

www.ksu.edu.sa
www.sciencedirect.com

ORIGINAL ARTICLE

Prediction of COVID-19 manipulation by selective ACE inhibitory compounds of *Potentilla reptant* root: *In silico* study and ADMET profile

Yuan Xu [a,*], Mahmood Al-Mualm [b], Ermias Mergia Terefe [c], Maksuda Ilyasovna Shamsutdinova [d], Maria Jade Catalan Opulencia [e], Fahad Alsaikhan [f], Abduladheem Turki Jalil [g], Ali Thaeer Hammid [h], Ayesheh Enayati [i,*], Hassan Mirzaei [i,*], Vahid Khori [i], Ali Jabbari [i], Aref Salehi [i,*], Alireza Soltani [j], Abdullah Mohamed [k]

[a] *First People's Hospital of Wuyi County, Zhejiang Province, Wuyi, Zhejiang 321200, China*
[b] *Department of Clinical Laboratory Techniques, Al-Nisour University College, Baghdad, Iraq*
[c] *School of Pharmacy and Health Science, United States International University, Nairobi, Kenya*
[d] *Department of Hematology, Transfusiology and Laboratory Affairs, Tashkent Medical Academy, Farobi Street 2, Tashkent 100109, Uzbekistan*
[e] *College of Business Administration, Ajman University, Ajman, United Arab Emirates*
[f] *College of Pharmacy, Prince Sattam Bin Abdulaziz University, Alkharj, Saudi Arabia*
[g] *Medical Laboratories Techniques Department, Al-Mustaqbal University College, Babylon, Hilla 51001, Iraq*
[h] *Computer Engineering Techniques Department, Faculty of Information Technology, Imam Ja'afar Al-Sadiq University, Baghdad, Iraq*
[i] *Ischemic Disorders Research Center, Golestan University of Medical Sciences, Gorgan, Iran*
[j] *Golestan Rheumatology Research Center, Golestan University of Medical Science, Gorgan, Iran*
[k] *Research Centre, Future University in Egypt, New Cairo 11845, Egypt*

Received 27 November 2021; accepted 21 April 2022
Available online 27 April 2022

KEYWORDS

COVID-19;
Potentilla reptans;
Angiotensin II;

Abstract In the novel SARS-CoV-2 (COVID-19) as a global emergency event, the main reason of the cardiac injury from COVID-19 is angiotensin-converting enzyme 2 (ACE2) targeting in SARS-CoV-2 infection. The inhibition of ACE2 induces an increase in the angiotensin II (Ang II) and the angiotensin II receptor type 1 (AT1R) leading to impaired cardiac function or cardiac inflammatory

* Corresponding authors.
E-mail addresses: xuyuan19870509@163.com (Y. Xu), Dr.enayati@goums.ac.ir (A. Enayati), mirzaei22@yahoo.com (H. Mirzaei), salehia@goums.ac.ir (A. Salehi).

Peer review under responsibility of King Saud University.

Production and hosting by Elsevier

https://doi.org/10.1016/j.arabjc.2022.103942

Molecular docking simulation;
ADMET

responses. The ethyl acetate fraction of *Potentilla reptans* L. root can rescue heart dysfunction, oxidative stress, cardiac arrhythmias and apoptosis. Therefore, isolated components of *P. reptans* evaluated to identify natural anti-SARS-CoV-2 agents via molecular docking.

In silico molecular docking study were carried out using the Auto Dock software on the isolated compounds of *Potentilla reptans* root. The protein targets of selective ACE and others obtained from Protein Data Bank (PDB). The best binding pose between amino acid residues involved in active site of the targets and compounds was discovered via molecular docking. Furthermore, ADMET properties of the compounds were evaluated.

The triterpenoids of *P. reptans* showed more ACE inhibitory potential than catechin in both domains. They were selective on the nACE domain, especially compound 5. Also, the compound 5 & 6 had the highest binding affinity toward active site of nACE, cACE, AT1R, ACE2, and TNF-α receptors. Meanwhile, compound 3 showed more activity to inhibit TXA2. Drug likeness and ADMET analysis showed that the compounds passed the criteria of drug likeness and Lipinski rules. The current study depicted that *P. reptans* root showed cardioprotective effect in COVID-19 infection and manipulation of angiotensin II-induced side effects.

1. Introduction

A novel coronavirus (SARS-CoV-2, COVID-19) has caused a great threat to the public healthcare systems and international concern in the world (Eftekhari et al., 2021a,b; Huang et al., 2020; Wang et al., 2020). This virus affected seriously endangers human health by causing susceptibility, disease severity, various mutations and high mortality (Fuzimoto and Isidoro, 2020; Hajikhani et al., 2020). As of now, there is not exact conventional medications for the SARS-CoV-2 treatment (Fuzimoto and Isidoro, 2020). It seems that there are several mechanisms involved in SARS-CoV-2 infection in different organs including lung, heart, kidney, and brain (Huang et al., 2020; Kannan et al., 2020). The main target of SARS-CoV-2 propagates is the angiotensin-converting enzyme 2 (ACE2) receptor and renin-angiotensin system (RAS) of host as a vehicle to entry human cells and viral replication (Pathangey et al., 2021). However, SARS-CoV-2 exhibits cardiac dysfunctions (owing to ACE2 abundant in cardiac tissue) including acute myocardial injury, hypokalemia, arrhythmia, myocarditis, and sudden cardiac death (Pathangey et al., 2021; Puelles et al., 2020; Tavazzi et al., 2020; Wichmann et al., 2020; Gupta et al., 2020). At that point, there is a specific attention to manage ACE2 expression or COVID-19 cardiac adverse and its associated targets such as cardiac inflammatory, Ang II induction, cardiac arrhythmia signaling and oxidative stress.

Viral binding to ACE2 leads to ACE2 shedding and an accumulation of Ang II and the angiotensin II receptor type 1 (AT1R), thereby causing an incidence of vasoconstriction, fibrosis, arrhythmogenesis, hypertrophy, proliferation, oxidative stress, cardiac dysfunction and myocardium sensitization (Pathangey et al., 2021; Bos et al., 2020; Liu et al., 2020). On the other hand, there is the relationship between elevated ACE2 and some cardiac comorbidities such as heart failure, secondary hypertension, coronary artery disease, and cardiomyopathies, which may increase COVID-19 susceptibility and severity (Pathangey et al., 2021). Likewise, angiotensin-I converting enzyme (ACE) inhibitors such as captopril, enalapril, and lisinopril are used to management of COVID-19 (Onweni et al., 2020). Owing to the non-selectivity of applied ACE inhibitors, they cause some side effects via associated dysregulatory of bradykinin in the patients (Caballero, 2020).

The many previous studies have indicated medicinal plants and natural products exert beneficial effects in treatment of COVID-19 (Din et al., 2020; Hashem-Dabaghian et al., 2021; Monfared et al., 2020), and also, they demonstrated the hopeful ACE inhibitory activity (Caballero, 2020). In this perspective, a growing body of evidence indicates that *Potentilla reptans* L. (Rosaceae) can rescue heart dysfunction, oxidative stress, cardiac arrhythmias and apoptosis through inhibiting ROS, glucocorticoid regulated kinase-1 (SGK1), glycogen synthase kinase 3β (GSK-3β), BAX and caspase3 regards to increasing Nrf2, SOD, CAT, NO, BCl-2 and improving cardiac hemodynamic function (Enayati et al., 2018, 2019, 2021a; Mudiyanselage et al., 2021; Antoine et al., 2022; Enayati et al., 2021b; Qi et al., 2022; Wu et al., 2021).

To the best our knowledge, *P. reptans*, as a natural cardioprotective agent may be a promising complementary candidate of COVID-19 for warrant therapeutic intention of ACE2 targeting-COVID-19-induced cardiac adverse. Therefore, we aimed to evaluate isolated components of *P. reptans* to identify natural anti-SARS-CoV-2 agents via molecular docking pointing the selective ACE inhibition and some properties including physicochemical, absorption, distribution, metabolism, excretion, and toxicity (ADMET).

2. Material and methods

2.1. Molecular docking

In this study, the anti-SARS-CoV-2 potential and the plausible selective-ACE inhibition (cACE or nACE domains) potential of *P. reptans* root compounds (Fig. 1) were investigated by *in silico* docking software Auto Dock (4.2) (Morris et al., 2009) on nACE-inhibition (PDB IDs: 6F9Vand 6EN5) and cACE-inhibition (PDB IDs: 1UZF, 2OC2, 6F9T and 6F9U) complexes (Caballero, 2020). Also, anti-inflammatory (PDB ID: 3KK6 and 2AZ5) and anti-thrombotic (PDB ID: 6IIU) effects of compounds were performed by molecular docking.

The 3D structure of targets obtained from PubChem database as following: the human testicular angiotensin I-

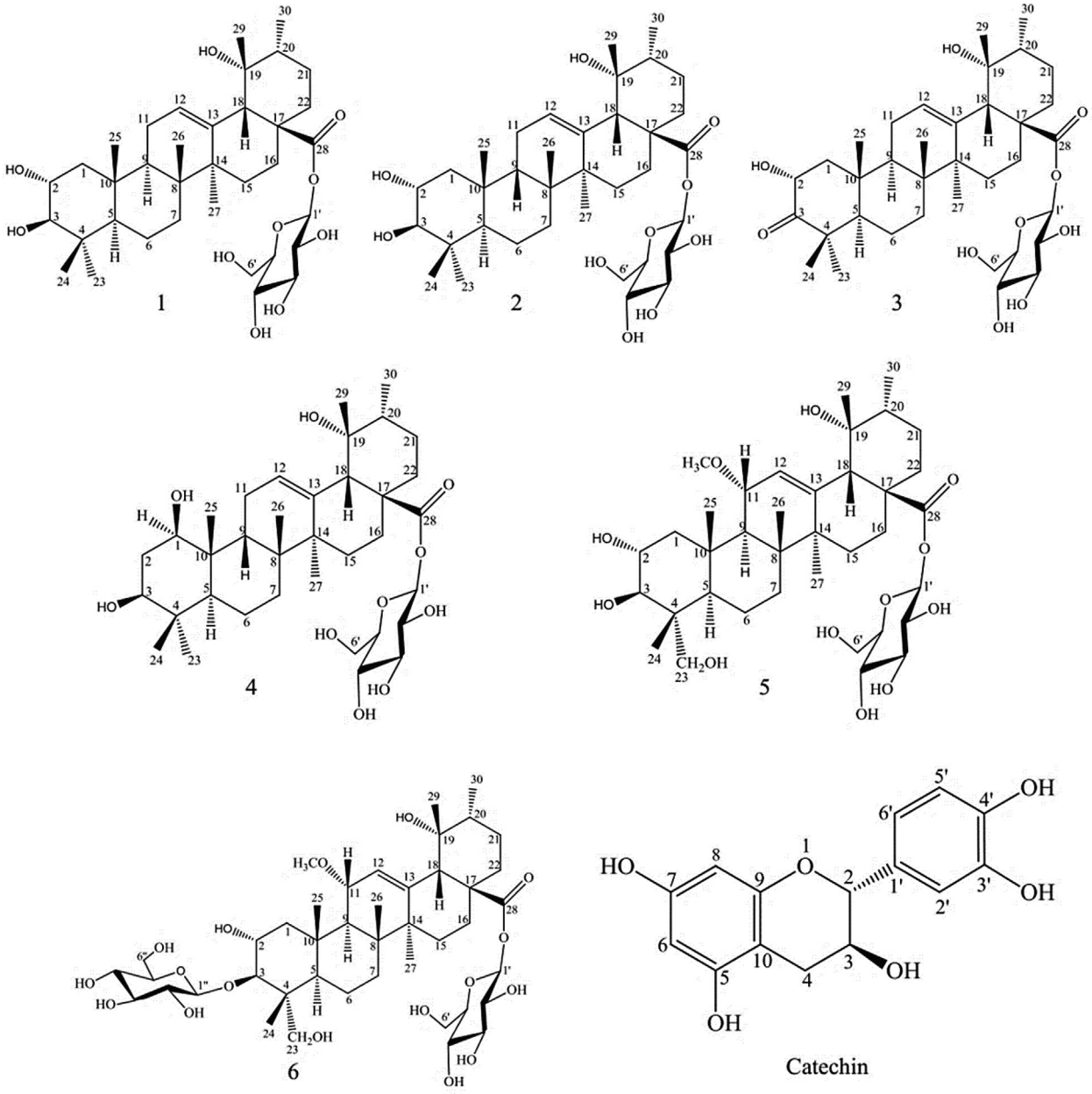

Fig. 1 Structures of isolated compounds from *P. reptans* root.

converting enzyme (cACE) (PDB ID: 1UZF), crystal structure of human angiotensin receptor in complex with inverse agonist olmesartan (AT1R) (PDB ID: 4ZUD), crystal structure of human angiotensin-1 converting enzyme N-domain in complex with sampatrilat (nACE) (PDB ID: 6F9V), crystal structure of human testis angiotensin-1 converting enzyme in complex with sampatrilat (cACE) (PDB ID: 6F9T), human testis Angiotensin-1 converting enzyme (cACE) (PDB ID: 6F9U), structure of testis ACE with RXPA380 (cACE) (PDB ID: 2OC2), crystal structure of the angiotensin-1 converting enzyme N-domain in complex with a diprolyl inhibitor (nACE) (PDB ID: 6EN5), structure of human angiotensin receptor inhibitor (AT1RI) (PDB ID: 4YAY), inhibitor bond human angiotensin converting enzyme-related carboxypeptidase (ACE2) (PDB ID: 1R4L), crystal structure of cyclooxygenase-1 in complex with celecoxib (COX-1) (PDB ID: 3KK6), crystal structure of the human thromboxane A2 receptor bond to ramatroban (TXA2) (PDB ID: 6IIU), crystal structure of TNF-alpha (TNF-α) (PDB ID: 2AZ5).

The docking was performed on the target proteins, which were removed water molecules/non-polar hydrogen atoms and added polar hydrogens/kollman charges (Pourbavarsad et al., 2021; Ma, 2020; Ma, 2021). Lamarckian genetic algorithm (GA) was used for local search method with a grid box of 60 × 60 × 60 and point spacing of 0.375 Å that was set for creating of autogrid module (Mirzaei et al., 2017; Emami et al., 2018). 150 GA runs were accomplished for each docking. Maestro 11.0 Schrodinger suit and Discovery Studio Visualizer software was applied for visualization of 2D and 3D presentation.

2.2. Ligand preparation

The 3D structure of each phytochemical (Fig. 1) was retrieved from PubChem database in SDF format and then converted into PDB format using Open Babel software. Chem3D software was utilized for energy minimization of ligands. Captopril, an ACE inhibitor not selective inhibitor, was used as a control.

2.3. Drug likeness and ADMET prediction

Efficacy and safety profile of the mentioned natural compounds including absorption, distribution, metabolism, excretion and toxicity (ADMET) and their pharmacokinetics were predicted using admetSAR database (Yang et al., 2019) and swissADME (Daina et al., 2017). Furthermore, we investigated topological polar surface area (TPSA) as an important descriptor predicting oral bioavailability and absorption of the compounds. Also, the compound effects on permeability of blood–brain barrier (BBB), inhibition of cytochrome P450 (CYP3A4, CYP2C9 and CYP2D6), AMES toxicity and carcinogenicity were evaluated.

3. Results

3.1. Molecular docking

According to Table 1, the triterpenoids of *P. reptans* showed more ACE inhibitory potential than catechin in both domains. Also, they were selective on the nACE domain based on their lower binding energies on 6F9V and 6EN5 targets, especially compound **5** had the lowest binding energy. Between assessed-PDB IDs of cACE domain, the triterpenoids revealed their lower binding energy in the binding pocket of 6F9U, mainly compound **6** (−10.2 kcal/mol), and also, it acted as more selective for cACE with lower binding energy for 6F9T and 2OC2 (as cACE domain complexes).

In addition, the results indicated that *P. reptans* root compounds are ACE inhibitor regards to the binding energy of ATR-inhibitor complexes 4YAY and 4ZUD, but compounds **5** and **6** showed suitable energy for ATR inhibition and acted as angiotensin receptor blocker (ARB). In ACE2 inhibitory investigation, triterpenoids were effective in the binding pocket of 1R4L protein especially compounds **5** and **2** (Table 1). In general, compounds **5** and **6** were more active in the inhibition of ACE, ACE2 and AT1R with their hydroxyl groups and electron donor –OMe substitution, thereby a preparation condition of interaction with the target Zn^{2+} ion.

In the present study, the compound **5** interacted with the 6F9V target in its active sites Cys330, Leu139, Phe490, Trp257, Phe435, Tyr498, Tyr501, Ala332, Tyr122 and Phe505 through hydrophobic interaction (Fig. 2A). Its polar interaction represented with residues Thr144, Arg350, Asp255, Lys489, His491, Ser260, Glu262, Asp393, Asp354, Glu431, and Ser504. Furthermore, hydroxyl and carbonyl groups of the compound **5** formed 11 hydrogen bonds with the amino acid residues Asp415, Asn277, His353, Cys352, Ala354, Thr372, Asp377 and Cys370 at the distances of 2.67, 3.04, 1.91, 2.62, 3.15, 1.78, 2.57, 2.77, 2.75, 2.62, and 2.66 Å, respectively (Fig. 2A). On the other hand, compound **5** interacted with the Zn^{2+} ion as essential element to binding the 6F9V target.

Fig. 2B illustrated hydrophobic interactions between the amino acid residues of target (6EN5) and compound **5**. In addition, the polar interactions with amino acid residues Asp140, Asp354, Arg350, Gln355, Glu389, Asp393, Ser504, Ser357, Thr358, His361, Lys432, His491, and Lys489 with compound **5** were indicated, that Thr358 interaction is important in nACE selectivity of compound **5** (Caballero, 2020). Furthermore, the compound **5** formed 8 hydrogen bonds with residues His331, Thr144, His491, Tyr498, Tyr501, Gln259, and Ser260 of 6EN5 target at 2.85, 2.96, 2.33, 1.89, 2.77, 2.23, 2.53 and 2.74 Å, respectively (Supplementary material Fig. S1). As illustrated in Fig. 2C-E, the compound **6** revealed selective cACE domain in the active site of targets (6F9U, 6F9T and 2OC2) through polar, hydrogen bond or hydrophobic interactions between important residues of targets with its hydroxyl, carbonyl and methoxyl groups (Supplementary material Figs. S2, S3, S4). Also, compound **6** and zinc atom of 6F9U interacted at 1.7 Å.

In the AT1R inhibitory analysis, compound **5** and **6** showed the lowest bonding energy in 4ZUD and 4YAY, respectively (Fig. 3A-B, Supplementary material Figs. S5, S6). In addition, the result of this study indicated the ACE2 inhibitory energy for compound **5** is −9.9 kcal/mol in the interaction with key

Table 1 Molecular docking simulation results for the compounds and receptors.

Compound	Binding Energy (kcal/mol) PDB ID:											
	1UZF (cACE)	**2OC2 (cACE)**	**6F9T (cACE)**	**6F9U (cACE)**	**6F9V (nACE)**	**6EN5 (nACE)**	**4YAY (AT1RI)**	**4ZUD (AT1R)**	**1R4L (ACE2)**	**3KK6 (COX-1)**	**6IIU (TXA2)**	**2AZ5 (TNF-α)**
Captopril	−7.6	−7.0	−7.1	−7.4	−7.3	−7.1	−7.1	−7.2	−7.6	−7.4	−7.3	−7.4
Catechin	−7.3	−7.2	−7.4	−7.7	−7.5	−7.6	−7.3	−7.3	−7.8	−7.8	−7.5	−7.5
1	−7.6	−7.8	−8.2	−8.7	−8.8	−8.3	−7.7	−7.7	−8.7	−7.3	−8.0	−7.9
2	−7.8	−7.6	−7.9	−9.5	−9.5	−9.1	−7.9	−7.8	−9.8	−7.1	−8.3	−8.1
3	−8.1	−8.7	−8.6	−9.2	−9.4	−9.2	−8.1	−8.0	−9.4	−7.7	−9.2	−8.2
4	−8.0	−8.5	−8.8	−9.0	−9.7	−9.7	−8.6	−8.2	−9.7	−7.5	−8.9	−8.5
5	−8.2	−8.3	−8.9	−9.6	−10.4	−9.8	−8.4	−9.4	−9.9	−8.3	−8.1	−8.3
6	−7.7	−9.3	−9.6	−10.2	−9.6	−9.6	−9.1	−8.6	−9.5	−6.3	−8.8	−8.6

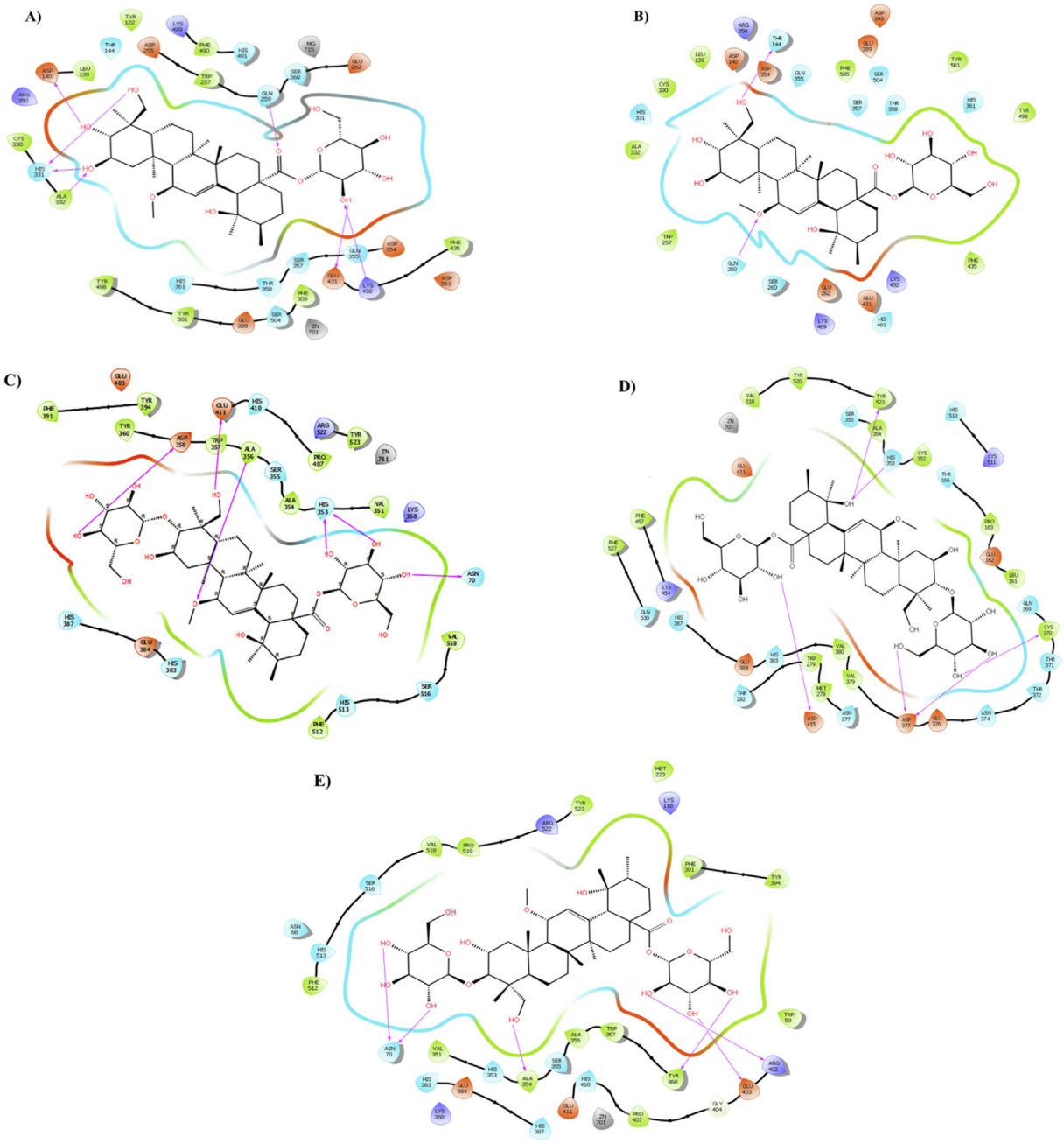

Fig. 2 Presentation of 2D model of interactions between compound **5** (A-B) and compound **6** (C-E) on selective ACE domains. A) Compound **5** and nACE (PDB ID:6F9V); B) Compound **5** and nACE (PDB ID:6EN5); C) Compound **6** and cACE (PDB ID: 6F9T); D) Compound **6** and cACE (PDB ID: 6F9U); E) Compound **6** and cACE (PDB ID: 2OC2).

amino acid residues of 1R4L and binding to Zn^{2+} ion at a distance of 2.9 Å (Fig. 3C, Table 1, Supplementary material Fig. S7).

As shown Table1, the compounds did not significantly inhibit COX-1. Compound **6** showed an inhibitory effect, more than other triterpenoids, on TNF-α (Fig. 4A, Supplementary material Fig. S8). In TXA2 inhibition compound **3** exerted binding affinity with residues Trp209 and Arg295 through its hydroxyl groups at 2.72 and 2.06 Å, respectively (Fig. 4B, Supplementary material Fig. S9).

3.2. Drug likeness and ADMET prediction

Pharmacokinetic and toxicity properties of compounds were determined. The results of predicted ADMET properties of compounds and toxicity profiles presented in Table 2.

To get an insight about the compliance of compounds with Lipinski's Rule of Five, the compounds screened for more analysis. Notably, most compounds passed Lipinski rule and did not show any violation of standardized Lipinski rule of five. Values of calculated solubility of compounds ranging

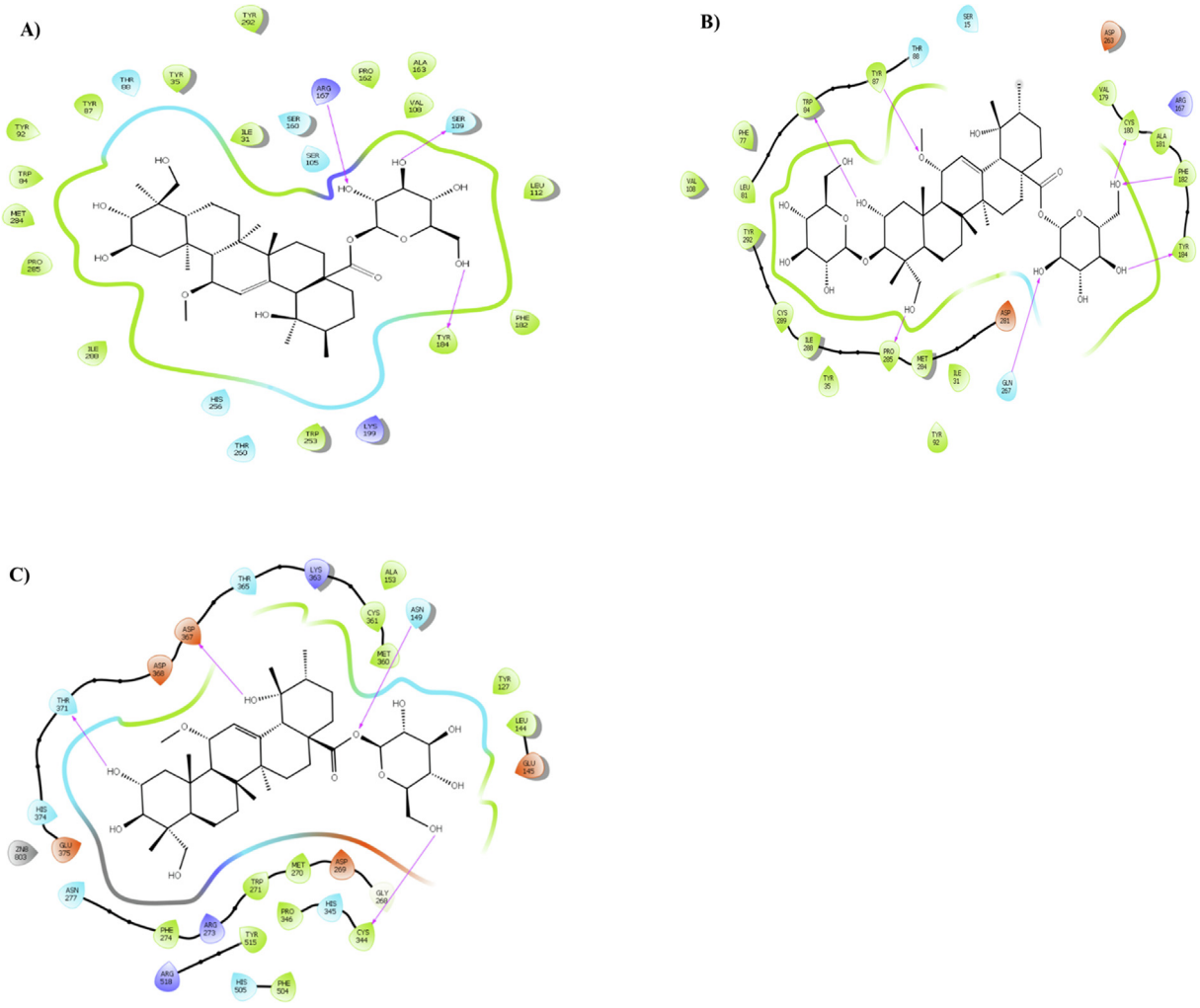

Fig. 3 Presentation of 2D model of interactions between A) compound **5** and AT1R (PDB ID: 4ZUD); B) compound **6** and (AT1R) (PDB ID: 4YAY); C) compound **5** and (ACE2) (PDB ID: 1R4L).

from −3.08 to −3.89 indicating moderate solubility of compounds, and also calculated Log P indicated between 1.29 and 3.26. Moreover, molecular weight was more than 500 Dalton, number of hydrogen bond donors were more than 5, while number of H-acceptors of compound **5** and **6** exhibited violation of Lipinski rule and others obey Lipinski rule (Obireddy and Lai, 2021; Andalib and Sarkar, 2021; Andalib and Sarkar, 2022; Alibak et al., 2022; Pelalak and Heidari, 2014).

Molar refractivity of all compounds were more than 130. According to data presented in Tables 2 and 3 pharmacokinetic parameters and ADMET profiles (absorption, distribution, metabolism, excretion, and toxicity) evaluated to predict the toxicity parameters of the compounds. However, all the compounds are following the criteria of drug likeness rules. All the compounds indicated good absorption and permeability demonstrating moderate absorption. Evaluation of two key ADMET descriptors like Human Intestinal Absorption (HIA) and blood brain barrier (BBB) exhibited appropriate profiles. Furthermore, the obtained results revealed that all of the compounds were non-inhibitors of CYP450 enzymes (3A4, 2D6, and 2C9) acting as an effective factor in drug metabolism (Wang et al., 2021; Dong et al., 2019; Huang et al., 2019; Huang et al., 2018; Jiang et al., 2021). Additionally, most compounds were non-carcinogenic, non-hepatotoxicity, and non-AMES toxicity.

4. Discussion

The previous studies established cardioprotective effects of *P. reptans* compounds in docking and animal experimental studies due to glycogen synthase kinase 3β (GSK-3β) and glucocorticoid regulated kinase-1 (SGK1) protein kinase inhibition (Enayati et al., 2021a; Enayati et al., 2021b). Likewise, they demonstrated an ischemic preconditioning property via antioxidant activity, nitric oxide release, activating Nrf2 pathway, and decreasing apoptotic markers in an isolated rat heart ischemia/reperfusion model (Enayati et al., 2018). Consistent with these data, *P. reptans* compounds may be applied for cardioprotection in COVID-19 by beneficial cardioprotective effects.

In this study, the isolated triterpenoids of *P. reptans* root showed selective ACE inhibitory effect as well as inhibition of ACE2 and AT1R, especially compound **5** and **6**, compared

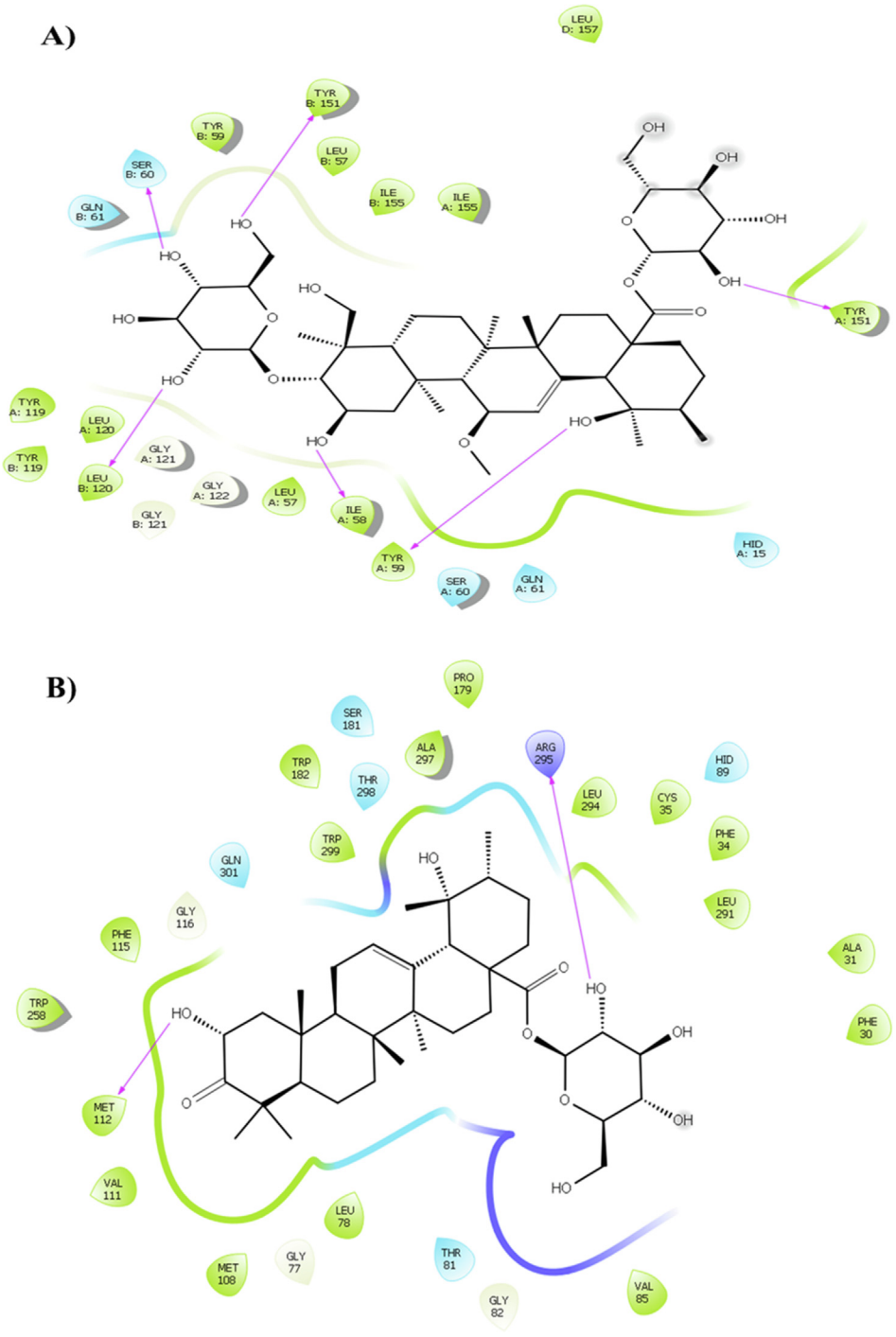

Fig. 4 Presentation of 2D model of interactions between A) compound **6** and (TNF-α) (PDB ID: 2AZ5); B) compound **3** and (TXA2) (PDB ID: 6IIU).

with catechin (Table 1). However, it may be explained by hydroxyl groups and electron donor substances in chemical structure of triterpenoids. In addition, the compound **5** and **6** had the highest binding affinity toward active site of nACE, cACE, AT1R, and ACE2 receptors, through -OMe element or hydroxyl groups. Also, their non-covalent (hydrogen bond and hydrophobic) interactions have a significant role in occupation of active site of the targets. Therefore, compound **5** and **6** can be considered as a potential selective ACE inhibitor by binding to the key amino acid residues in the active site of the targets.

To the best of our knowledge, the selective inhibition of ACE plays a pivotal role in controlling the RAS and kallikrein-kinin system (KKS), thereby normal hydrolyzing of the anti-inflammatory peptide N-acetyl-SDKP and bradykinin by nACE and cACE, respectively. Therefore, selective cACE inhibitors diminish the production of angiotensin-II

Table 2 Drug-likeness properties of compounds.

Compound	MW	Log S	C log P	HBA	HBD	NRB	MR	TPSA
Ref.	–	> -4	< = 5	< = 10	< = 5	< = 10	40–130	< 140
1	650	−3.71	3.2	10	7	4	171	177
2	650	−3.86	2.43	10	7	4	171	177
3	648	−3.76	3.26	10	6	4	170	173
4	650	−3.89	3.22	10	7	4	171	177
5	696	−3.61	2.06	12	8	6	178	206
6	858	−3.08	1.29	17	11	9	209	285
Catechin	290	−2.73	1.34	6	5	1	74	110
Captopril	217	−0.06	0.27	4	1	4	60	57

HBA: Number of hydrogen bonds acceptors; **HBD:** Number of hydrogen bond donors; **Log S:** Logarithm of water solubility; **C Log P:** Calculated logarithm of compound partition coefficient between n-octanol and water; **MR:** Molecular refractivity; **MW:** molecular weight; **NRB:** Number of rotatable bonds; **TPSA:** Topological polar surface area.

Table 3 ADMET (absorption, distribution, metabolism, excretion and toxicity) profile of compounds.

Compound	BBB	HIA	Caco2	P-GI	CYP450-2C9	CYP450-2D6	CYP450-3A4	AMES	CIG	HPT	AOC
Ref.	–	–	–	No	No	No	No	No	No	No	–
1	No	Yes	No	Yes	No	No	No	No	No	No	3.1
2	No	Yes	No	Yes	No	No	No	No	No	No	3.1
3	No	Yes	No	Yes	No	No	No	No	No	No	3.2
4	No	Yes	No	Yes	No	No	No	No	No	No	3.5
5	No	Yes	No	Yes	No	No	No	No	No	No	3.0
6	No	No	No	Yes	No	No	No	No	No	No	3.3
Catechin	No	Yes	No	No	No	No	No	No	No	No	2.0
Captopril	Yes	Yes	No	No	Yes	No	No	No	No	No	1.8

AOC: Acute oral toxicity; **BBB:** Blood Brain Barrier; **CIG:** Carcinogens; **HIA:** Human Intestinal Absorption; **HPT:** Hepatotoxicity; **P-GI:** P-glycoprotein inhibitor. **Caco2:** A model of the intestinal epithelial barrier**; AMES:** To assess the mutagenic potential of chemical compounds.

(AngII), ACE2 and plausible angioedema. On the other hand, selective nACE inhibitors attenuate inflammation and fibrosis of heart, renal and vascular through increasing N-acetyl-SDKP levels (Caballero, 2020; Bernstein et al., 2011). However, selective ACE inhibitors prevent the activity of cACE or nACE domains.

It seems that AT1R and ACE2 inhibitory effects of *P. reptans* triterpenoids (as shown Table 1) can explain their suppressing effects in inflammatory and cardiac fibrosis induced by COVID-19 infection and dysfunction in RAS. It has been reported that AngII induced angiotensin II type-2 receptor (AT2R) and NO production when AT1R blocked and leads to cardioprotection and anti-fibrosis via inhibiting of norepinephrine, MAPK and ERK1/2 along with inducing vasodilation by bradykinin/NO/cGMP cascades (Yosofvand et al., 2020; Jalalieh et al., 2021; Niknam et al., 2021; Pourbavarsad et al., 2022). In addition, the previous studies indicated that isolated ingredients of *P. reptans* inhibited cardiac apoptosis via NO release, inhibiting GSK-3β and activating RISK/SAFE pathways in reperfusion injury (Enayati et al., 2021b). On the other hand, AT1R inhibition may upregulate ACE2 levels as important target of SARS-CoV-2 (Onweni et al., 2020), thereby the *P. reptans* compounds can exert a protective role against an increase in ACE2 by their affinity to occupation of ACE2 complex.

In the next step, the current study demonstrated that compounds of *P. reptans* inhibited TXA2 and TNF-α (Table 1) as adverse effects of infection with COVID-19, which can be in line with mentioned properties of compounds and explain by their antioxidant and anti-inflammatory or anti-apoptotic effects (Enayati et al., 2018; Enayati et al., 2021b). Furthermore, the recent study reported that AngII acts similar to inflammatory cytokine and induces hypertrophy, fibrosis, arterial fibrillation and arrhythmia in the heart (Li et al., 2012). Likewise, it can activate numerous kinases such as SGK1 that plays a pivotal dual role in the pathogenesis of cardiac arrhythmia, inflammation and remodeling in response to progressive elevated AngII (Forrester et al., 2018; Gan et al., 2018). Agreeing with this evidence, ethyl acetate fraction of *P. reptans* exerted inhibitory effects on SGK1 to reduce arrhythmia and cardiac apoptosis in ischemia/reperfusion injury (Enayati et al., 2021a; Enayati et al., 2021b). However, AngII and AT1R could cause arterial/ventricular fibrillation, thus, by blocking ACE or AT1R it would be plausible that inhibition of SGK1 to reduce the prolongation of the action potential duration (APD), hypokalemia, and the proarrhythmic effects of AngII (Goette and Lendeckel, 2008). Therefore, *Potentilla reptans* compounds may be promising candidate as anti-arrhythmic agent for management of ACE2 targeting-COVID-19-induced arrhythmia due to their ACE or AT1R inhibitory properties.

Taken together, isolated substance of ethyl acetate fraction of *P. reptans* root showed cardioprotective effect in COVID-19 infection and manipulation of angiotensin II-induced side

effects by molecular docking which can be postulated as new selective ACE inhibitors. Although ethyl acetate fraction of *P. reptans* root showed beneficial pharmacological properties in the management of COVID-19 and its adverse effects, larger preclinical and clinical studies are needed to determine whether the compounds reveal safety and selective ACE that indicated by molecular docking.

5. Conclusions

In conclusion, the molecular docking results of present study gave insights into the potential efficacy of triterpenoid compounds from *P. reptans* root against COVID-19 through selective ACE inhibitory effect, AT1R and ACE2 inhibition. Ursane type triterpenoids and catechins of *P. reptans*, especially compound **5** and **6**, seems to contribute to anti-COVID-19 and cardioprotective effects of this plant in the *in silico*. Our findings indicate that *P. reptans* compounds follow Lipinski rule of five and had good pharmacokinetic properties and ADMET profiles. However, further studies in animal and clinical areas in an enhanced setting, are needed to indicate other promising targets and mechanisms of anti-COVID-19 from *Potentilla reptans* root ingredients. Finally, it can be a hopeful natural-based approach for demoliting the pathogenesis of COVID-19 and boosted AngII.

Acknowledgments

This article financially supported by Golestan University of Medical Sciences, Gorgan, Iran (IR.GOUMS.REC.1400.107).

Appendix A. Supplementary material

Supplementary data to this article can be found online at https://doi.org/10.1016/j.arabjc.2022.103942.

References

Alibak, A.H., Khodarahmi, M., Fayyazsanavi, P., Alizadeh, S.M., Hadi, A.J., Aminzadehsarikhanbeglou, E., 2022. Simulation the adsorption capacity of polyvinyl alcohol/carboxymethyl cellulose based hydrogels towards methylene blue in aqueous solutions using cascade correlation neural network (CCNN) technique. J. Cleaner Prod. 130509

Andalib, V., Sarkar, J., 2021. A repairable system supported by two spare units and serviced by two types of repairers. J. Stat. Theory Appl. 20 (2), 180–192.

Andalib, V., Sarkar, J., 2022. A system with two spare units, two repair facilities, and two types of repairers. Mathematics 10 (6), 852.

Antoine, D., Mohammadi, M., Vitt, M., Dickie, J.M., Jyoti, S.S., Tilbury, M.A., ... Wall, J.G., 2022. Rapid, point-of-care scFv-SERS assay for femtogram level detection of SARS-CoV-2. ACS Sens. Available from: <https://pubs.acs.org/doi/10.1021/acssensors.1c02664>.

Bernstein, K.E., Shen, X.Z., Gonzalez-Villalobos, R.A., Billet, S., Okwan-Duodu, D., Ong, F.S., Fuchs, S., 2011. Different in vivo functions of the two catalytic domains of angiotensin-converting enzyme (ACE). Curr. Opin. Pharmacol. 11 (2), 105–111.

Bos, J.M., Hebl, V.B., Oberg, A.L., Sun, Z., Herman, D.S., Teekakirikul, P., Seidman, J.G., Seidman, C.E., Dos Remedios, C.G., Maleszewski, J.J., Schaff, H.V., 2020. Marked up-regulation of ACE2 in hearts of patients with obstructive hypertrophic cardiomyopathy: implications for SARS-CoV-2–mediated COVID-19. Mayo Clin. Proc. 95, 1354–1368.

Caballero, J., 2020. Considerations for docking of selective angiotensin-converting enzyme inhibitors. Molecules 25 (2), 295.

Daina, A., Michielin, O., Zoete, V., 2017. SwissADME: a free web tool to evaluate pharmacokinetics, drug-likeness and medicinal chemistry friendliness of small molecules. Sci. Rep. (Sci. Rep.) 7 (1), 1–3.

Din, M., Ali, F., Waris, A., Zia, F., Ali, M., 2020. Phytotherapeutic options for the treatment of COVID-19: a concise viewpoint. Phytother. Res., 1–7

Dong, H., Zheng, L., Yu, P., Jiang, Q., Wu, Y., Huang, C., Yin, B., 2019. Characterization and application of lignin–carbohydrate complexes from lignocellulosic materials as antioxidants for scavenging in vitro and in vivo reactive oxygen species. ACS Sustainable Chem. Eng. 8 (1), 256–266.

Eftekhari, M., Enayati, A., Doustimotlagh, A.H., Farzaei, M.H., Yosifova, A.I., 2021a. Natural products in combination therapy for COVID-19: QT prolongation and urgent guidance. Nat. Prod. Commun. 16 (9). 1934578X211032471.

Eftekhari, M., Salehi, A., Enayati, A., 2021b. Management of COVID-19 by phytotherapy: a pharmacological viewpoint. J. Rep. Pharm. Sci. 10 (1), 153.

Emami, S., Esmaili, Z., Dehghan, G., Bahmani, M., Hashemi, S.M., Mirzaei, H., Shokrzadeh, M., Moradi, S.E., 2018. Acetophenone benzoylhydrazones as antioxidant agents: synthesis, in vitro evaluation and structure-activity relationship studies. Food Chem. (Food Chem.) 268, 292–299.

Enayati, A., Salehi, A., Alilou, M., Stuppner, H., Mirzaei, H., Omraninava, A., Khori, V., Yassa, N., 2021a. Six new triterpenoids from the root of *Potentilla reptans* and their cardioprotective effects *in silico*. Nat. Prod. Res. 1–9.

Enayati, A., Yassa, N., Mazaheri, Z., Rajaei, M., Pourabouk, M., Ghorghanlu, S., Basiri, S., Khori, V., 2018. Cardioprotective and anti-apoptotic effects of *Potentilla reptans* L. root via Nrf2 pathway in an isolated rat heart ischemia/reperfusion model. Life Sci. 215, 216–226.

Enayati, A., Khori, V., Saeedi, Y., Yassa, N., 2019. Antioxidant activity and cardioprotective effect of *Potentilla Reptans* L. via ischemic preconditioning (IPC). RJP 6 (1), 19–27.

Forrester, S.J., Booz, G.W., Sigmund, C.D., Coffman, T.M., Kawai, T., Rizzo, V., Scalia, R., Eguchi, S., 2018. Angiotensin II signal transduction: an update on mechanisms of physiology and pathophysiology. Physiol. Rev. 98 (3), 1627–1738.

Fuzimoto, A.D., Isidoro, C., 2020. The antiviral and coronavirus-host protein pathways inhibiting properties of herbs and natural compounds-additional weapons in the fight against the COVID-19 pandemic? J. Tradit. Complement. Med. 10 (4), 405–419.

Enayati, A., Salehi, A., Alilou, M., Stuppner, H., Polshekan, M., Rajaei, M., Pourabouk, M., Jabbari, A., Mazaheri, Z., Yassa, N., Moheimani, H.R., Khori, V. 2021b. *Potentilla reptans* L. Postconditioning Protects Reperfusion Injury Via The RISK/SAFE Pathways in an Isolated Rat Heart. doi: 10.21203/rs.3.rs-148595/v1.

Gan, W., Ren, J., Li, T., Lv, S., Li, C., Liu, Z., Yang, M., 2018. The SGK1 inhibitor EMD638683, prevents Angiotensin II–induced cardiac inflammation and fibrosis by blocking NLRP3 inflammasome activation. Biochim. Biophys. Acta (BBA)-Molecular Basis of Disease (BBA-MOL BASIS DIS) 1864 (1), 1–0.

Goette, A., Lendeckel, U., 2008. Electrophysiological effects of angiotensin II. Part I: signal transduction and basic electrophysiological mechanisms. Europace 10 (2), 238–241.

Gupta, A., Madhavan, M.V., Sehgal, K., Nair, N., Mahajan, S., Sehrawat, T.S., Bikdeli, B., Ahluwalia, N., Ausiello, J.C., Wan, E. Y., Freedberg, D.E., 2020. Extrapulmonary manifestations of COVID-19. Nat. Med. 26 (7), 1017–1032.

Hajikhani, B., Calcagno, T., Nasiri, M.J., Jamshidi, P., Dadashi, M., Goudarzi, M., Eshraghi, A.A., FACS, Mirsaeidi, M., 2020. Olfactory and gustatory dysfunction in COVID-19 patients: a meta-analysis study. Physiol. Rep. 8 (18), e14578.

Hashem-Dabaghian, F., Zimi, S.A., Bahrami, M., Latifi, S.A., Enayati, A., Qaraaty, M., 2021. Effect of Lavender (Lavandula angustifolia L.) syrup on olfactory dysfunction in COVID-19 infection: a pilot controlled clinical trial. Avicenna J. Phytomed. (AJP).

Huang, C., Tang, S., Zhang, W., Tao, Y., Lai, C., Li, X., Yong, Q., 2018. Unveiling the structural properties of lignin–carbohydrate complexes in bamboo residues and its functionality as antioxidants and immunostimulants. ACS Sustainable Chem. Eng. 6 (9), 12522–12531.

Huang, C., Su, Y., Shi, J., Yuan, C., Zhai, S., Yong, Q., 2019. Revealing the effects of centuries of ageing on the chemical structural features of lignin in archaeological fir woods. New J. Chem. 43 (8), 3520–3528.

Huang, C., Wang, Y., Li, X., Ren, L., Zhao, J., Hu, Y., Zhang, L., Fan, G., Xu, J., Gu, X., Cheng, Z., 2020. Clinical features of patients infected with 2019 novel coronavirus in Wuhan, China. Lancet 395 (10223), 497–506.

Jalalieh, B.J., Jackson, W.A., Cumbie, B., Pourbavarsad, M.S., 2021, July. Organic carbon and nitrogen removal in a single-stage nitrification-denitrification/anammox (NDX) system treating early planetary base (EPB) wastewater. In: 50th International Conference on Environmental Systems.

Jiang, J., Zhang, T., Chen, D., 2021. Analysis, design, and implementation of a differential power processing DMPPT with multiple buck–boost choppers for photovoltaic module. IEEE Trans. Power Electron. 36 (9), 10214–10223.

Kannan, S.P., Ali, P.S., Sheeza, A., Hemalatha, K., 2020. COVID-19 (Novel Coronavirus 2019)-recent trends. Eur. Rev. Med. Pharmacol. Sci. 24 (4), 2006–2011.

Li, Y., Li, X.H., Yuan, H., 2012. Angiotensin II type-2 receptor-specific effects on the cardiovascular system. Cardiovasc. Diagn. Ther. 2 (1), 56.

Liu, P.P., Blet, A., Smyth, D., Li, H., 2020. The science underlying COVID-19: implications for the cardiovascular system. Circulation 142 (1), 68–78.

Ma, W., 2020 (2020). Nonlinear analysis of progressive collapse of reinforced concrete (RC) building by different kinds of column removal. Front. Res. Archit. Eng. 3 (1).

Ma, W., 2021. Behavior of Aged Reinforced Concrete Columns under High Sustained Concentric and Eccentric Loads (Doctoral dissertation, University of Nevada, Las Vegas).

Mirzaei, H., Shokrzadeh, M., Emami, S., 2017. Synthesis, cytotoxic activity and docking study of two indole-chalcone derivatives. J. Mazandaran Univ. Med. Sci. (J. Maz. Univ. Med. Sci.) 27 (154), 12–25.

Monfared, M., Eftekhari, M., Enayati, A., Sabeti, M., Amini, M.H., 2020. COVID-19 disease management from the perspective of Traditional Persian Medicine. J. Islamic Iran. Trad. Med. (JIITM) 11 (1), 11–22.

Morris, G.M., Huey, R., Lindstrom, W., Sanner, M.F., Belew, R.K., Goodsell, D.S., Olson, A.J., 2009. AutoDock4 and AutoDockTools4: automated docking with selective receptor flexibility. J. Comput. Chem. (J. Comput. Chem.) 30 (16), 2785–2791.

Mudiyanselage, S.E., Nguyen, P.H.D., Rajabi, M.S., Akhavian, R., 2021. Automated workers' ergonomic risk assessment in manual material handling using sEMG wearable sensors and machine learning. Electronics 10 (20), 2558.

Niknam, B., Aboutalebi, F.H., Ma, W., Nejad, R.M., 2021. Effect of variations internal pressure on cracking radiant coils distortion. Structures 34, 4986–4998.

Obireddy, S.R., Lai, W., 2021. Preparation and characterization of 2-hydroxyethyl starch microparticles for co-delivery of multiple bioactive agents. Drug Delivery 28 (1), 1562–1568.

Onweni, C.L., Zhang, Y.S., Caulfield, T., Hopkins, C.E., Fairweather, D.L., Freeman, W.D., 2020. ACEI/ARB therapy in COVID-19: the double-edged sword of ACE2 and SARS-CoV-2 viral docking. Crit. Care 24 (1), 1–3.

Pathangey, G., Fadadu, P.P., Hospodar, A.R., Abbas, A.E., 2021. Angiotensin-converting enzyme 2 and COVID-19: patients, comorbidities, and therapies. Am. J. Physiol. Lung Cell Mol. Physiol. 320 (3), L301–L330.

Pelalak, R., Heidari, Z., 2014. Lithographically cut multiwalled carbon nanotubes: opening caps, controlling length distribution, and functionalization. J. Dispersion Sci. Technol. 35 (6), 808–814.

Pourbavarsad, M.S., Jalalieh, B.J., Harkins, C., Sevanthi, R., Jackson, W.A., 2021. Nitrogen oxidation and carbon removal from high strength nitrogen habitation wastewater with nitrification in membrane aerated biological reactors. J. Environ. Chem. Eng. 9, (5) 106271.

Pourbavarsad, M.S., Jalalieh, B.J., Landes, N., Jackson, W.A., 2022. Impact of free ammonia and free nitrous acid on nitritation in membrane aerated bioreactors fed with high strength nitrogen urine dominated wastewater. J. Environ. Chem. Eng. 10, (1) 107001.

Puelles, V.G., Lütgehetmann, M., Lindenmeyer, M.T., Sperhake, J.P., Wong, M.N., Allweiss, L., Chilla, S., Heinemann, A., Wanner, N., Liu, S., Braun, F., 2020. Multiorgan and renal tropism of SARS-CoV-2. N. Engl. J. Med. 383 (6), 590–592.

Qi, H., Hu, Z., Yang, Z., Zhang, J., Wu, J.J., Cheng, C.,... Zheng, L., 2022. Capacitive aptasensor coupled with microfluidic enrichment for real-time detection of trace SARS-CoV-2 nucleocapsid protein. Anal. Chem. (Washington). doi: 10.1021/acs.analchem.1c04296.

Tavazzi, G., Pellegrini, C., Maurelli, M., Belliato, M., Sciutti, F., Bottazzi, A., Sepe, P.A., Resasco, T., Camporotondo, R., Bruno, R., Baldanti, F., 2020. Myocardial localization of coronavirus in COVID-19 cardiogenic shock. Eur. J. Heart Fail. 22 (5), 911–915.

Wang, C., Horby, P.W., Hayden, F.G.G.G., 2020. A novel coronavirus outbreak of global health concern. Lancet 395 (10223), 470–473.

Wang, X., Tang, S., Chai, S., Wang, P., Qin, J., Pei, W., Huang, C., 2021. Preparing printable bacterial cellulose based gelatin gel to promote in vivo bone regeneration. Carbohydr. Polym. 270, 118342.

Wichmann, D., Sperhake, J.P., Lütgehetmann, M., Steurer, S., Edler, C., Heinemann, A., Heinrich, F., Mushumba, H., Kniep, I., Schröder, A.S., Burdelski, C., 2020. Autopsy findings and venous thromboembolism in patients with COVID-19: a prospective cohort study. Ann. Intern. Med. 173 (4), 268–277.

Wu, S., Zhang, K., Parks-Stamm, E.J., Hu, Z., Ji, Y.,... Cui, X., Increases in anxiety and depression during COVID-19: a large longitudinal study from China. Front. Psychol. 12 (2021) 706601.

Yang, H., Lou, C., Sun, L., Li, J., Cai, Y., Wang, Z., Li, W., Liu, G., Tang, Y., 2019. admetSAR 2.0: web-service for prediction and optimization of chemical ADMET properties. Bioinformatics (Bioinform.) 35 (6), 1067–1069.

Yosofvand, M., Liyanage, S., Kalupahana, N.S., Scoggin, S., Moustaid-Moussa, N., Moussa, H., 2020. AdipoGauge software for analysis of biological microscopic images. Adipocyte 9 (1), 360–373.